Journal of Power Sources 328 (2016) 124–135

Contents lists available at ScienceDirect

Journal of Power Sources

journal homepage: www.elsevier.com/locate/jpowsour

Enabling linear alkyl carbonate electrolytes for high voltage Li-ion cells

Jian Xia [a], Remi Petibon [b], Deijun Xiong [b], Lin Ma [b], J.R. Dahn [a, b, *]

[a] Dept. of Physics and Atmospheric Science, Dalhousie University, Halifax, Nova Scotia, B3H3J5, Canada
[b] Dept. of Chemistry, Dalhousie University, Halifax, Nova Scotia, B3H4R2, Canada

HIGHLIGHTS

- Ethylene carbonate (EC) is actually detrimental for Li-ion cells at high voltages.
- EC-free linear alkyl carbonate electrolytes with various “enablers” were developed.
- Linear alkyl carbonate electrolytes have very good performance at high voltages.

ARTICLE INFO

Article history:
Received 20 June 2016
Received in revised form
17 July 2016
Accepted 2 August 2016
Available online 9 August 2016

Keywords:
Linear alkyl carbonates
EC-free electrolytes
High voltage Li-ion cells
Passivating additives
Ethyl methyl carbonate plus fluoroethylene carbonate

ABSTRACT

Some of the problems of current electrolytes for high voltage Li-ion cells originate from ethylene carbonate (EC) which is thought to be an essential electrolyte component for Li-ion cells. Ethylene carbonate-free electrolytes containing 1 M $LiPF_6$ in ethylmethyl carbonate (EMC) with small loadings of vinylene carbonate, fluoroethylene carbonate, or (4R,5S)-4,5-Difluoro-1,3-dioxolan-2-one acting as “enablers” were developed. These electrolytes used in $Li(Ni_{0.4}Mn_{0.4}Co_{0.2})O_2$/graphite pouch type Li-ion cells tested at 4.2 V and 4.5 V yielded excellent charge-discharge cycling and storage properties. The results for cells containing linear alkyl carbonate electrolytes with no EC were compared to those of cells with EC-containing electrolytes incorporating additives proven to enhance cyclability of cells. The combination of EMC with appropriate amounts of these enablers yields cells with better performance than cells with EC-containing electrolytes incorporating additives tested to 4.5 V. Further optimizing these linear alkyl carbonate electrolytes with appropriate co-additives may represent a viable path to the successful commercial utilization of NMC/graphite Li-ion cells operated to 4.5 V and above.

1. Introduction

Li-ion batteries (LiBs) with higher energy density as well as longer lifetime are desired for applications such as portable consumer electronics, electric vehicles (EVs) and grid energy storage [1,2]. While the energy density generally relies on the selection of electrode materials, the lifetime depends heavily on the choice of electrolyte. Over the past few decades, a variety of electrode materials have been developed and commercialized [3–10]. However, the commercialization of new electrolyte solvents has been relatively slow. Currently, state-of-the-art electrolytes are very similar to the ones used twenty five years ago. These are based on mixtures containing $LiPF_6$, ethylene carbonate (EC), sometimes propylene carbonate (PC) and linear carbonates selected from ethyl methyl carbonate (EMC), dimethyl carbonate (DMC) and diethyl carbonate (DEC). A wide variety of electrolyte additives, such as vinylene carbonate (VC) [11] and biphenyl [12], are incorporated to improve battery lifetime and response to electrical abuse, respectively. The cycling performance of Li-ion cells with these carbonate based electrolytes has been poor at or above 4.4 V due to increased electrolyte oxidation at the surface of positive electrode as the potential increases. The degradation of these electrolyte components at high voltages results in salt consumption, gas evolution and impedance growth, which reduce the energy density and the lifetime of Li-ion cells [13–16].

New alternative electrolyte formulations with high anodic stability are needed. Several organic compounds with strong electron-withdrawing groups, such as sulfones [17,18], nitriles [19,20], ionic

* Corresponding author. Dept. of Physics and Atmospheric Science, Dalhousie University, Halifax, Nova Scotia, B3H3J5, Canada.
E-mail address: jeff.dahn@dal.ca (J.R. Dahn).

http://dx.doi.org/10.1016/j.jpowsour.2016.08.015
0378-7753/

liquids [21–24] and fluorinated compounds [25–28] are reported to have excellent anodic stability and have been studied as electrolyte solvents for high voltage Li-ion cells. However, many of these organic compounds which have high oxidation stability do not provide a good passivation at the graphite electrode without EC as a co-solvent. Moreover, problems associated with solubility with salt, toxicity, cost and safety must be addressed before these solvents are widely used in Li-ion cells [29,30].

It is thought that EC is essential for the passivation of the graphite electrodes surface during the first cycle [31,32]. However, left-over EC in the electrolyte may be continuously oxidized at the positive electrode in cells operated to high voltage. This may lead to gas generation and impedance growth. It was recently shown that the removal of EC from carbonate-based electrolytes yielded high voltage Li-ion cells with longer life-time [33]. EC-free-linear alkyl carbonate-based electrolytes with a small amount of "enabler", namely vinylene carbonate (VC), allowed NMC(442)/graphite cells to be cycled up to 4.4 V with longer cycle and calendar life, compared to cells with a state-of-the-art electrolyte incorporating additives [33]. For instance, NMC(442)/graphite cells filled with 1 M $LiPF_6$ EMC:VC (98:2) + 2% PPF (pyridine phosphorus pentafluoride) were shown to have longer cycle life at both room temperature and 55 °C when cycled up to 4.4 V than cells with EC-based electrolytes incorporating state of the art additive blends [33]. The EMC:VC (98:2) electrolyte system also has acceptable conductivity, wets separators quickly, shows good tolerance to high voltage and provides cells with low polarization growth when cycled up to 4.4 V.

SEI forming additives other than VC, such as fluoroethylene carbonate (FEC), (4R,5S)-4,5-Difluoro-1,3-dioxolan-2-one (DiFEC) [34], methylene-ethylene carbonate (MEC) [35], prop-1-ene-1,3-sultone (PES) [36] and succinic anhydride (SA) [37] are also effective "enablers" for $Li[Ni_{0.4}Mn_{0.4}Co_{0.2}]O_2$ (NMC442)/graphite pouch cells containing linear alkyl carbonate-based electrolytes cycled to high voltages. Fig. 1 and Fig. S1 (supporting information) show the structure of various additives and differential capacity (dQ/dV) *vs.* voltage (V) curves for the first charge (formation cycle) of NMC442/graphite pouch cells filled with EMC-based electrolytes to which various additives have been added. Fig. 1 and Fig. S1 show that cells which do not contain any additives have a large reduction peak around 3.2 V. This peak corresponds to the reduction of EMC and is associated with the generation of a large volume of gas (around 2 mL corresponding to 100% cell expansion). Fig. 1 and Fig. S1 clearly show that enablers such as VC, FEC, DiFEC, PES, SA and MEC can greatly suppress the reduction peak of EMC at 3.2 V (graphite around 0.45 V vs. Li/Li^+) while other additives such as vinyl ethylene carbonate (VEC), maleic anhydride (MA) and diphenyl carbonate (DPC) cannot. The amount of enabler is also critical. For instance, Fig. S2a shows that a low concentration of SA such as 0.2% or 0.5% is not enough to suppress the reduction peak of EMC while higher concentrations such as 1% can totally suppress the reduction peak of EMC. However, for additives such as VEC (see Fig. S2b), even with 4%, the reduction peak of EMC cannot be suppressed. Table 1 shows a summary of additives that can successfully passivate the graphite electrode, when used with linear alkyl carbonate solvents alone.

In this paper, four "enablers" including EC, VC, FEC and DiFEC were compared head to head in NMC442/graphite pouch type Li-ion cells. Other enablers such as SA, MEC, PES will not be included in this paper but will be discussed in latter publications. Experiments were made using ultra high precision coulometry (UHPC) [38], a precision storage system [39],electrochemical impedance spectroscopy (EIS) and a gas measurement. Gas evolution during formation and cycling, coulombic efficiency, charge endpoint capacity slippage during cycling and EIS spectra before and after cycling were examined and were compared to EC-based electrolyte with some promising additive blends.

2. Experimental

2.1. Chemicals

1 M $LiPF_6$ in ethylene carbonate (EC):ethyl methyl carbonate (EMC) 3:7 wt% ratio, (BASF - $LiPF_6$, purity 99.94%, water content 14 ppm; EC:EMC, 3:7 by weight, water content < 20 ppm) was used as the control electrolyte. Electrolyte blends based on 1 M $LiPF_6$ in EMC were also studied. To the EMC-based electrolyte, additives

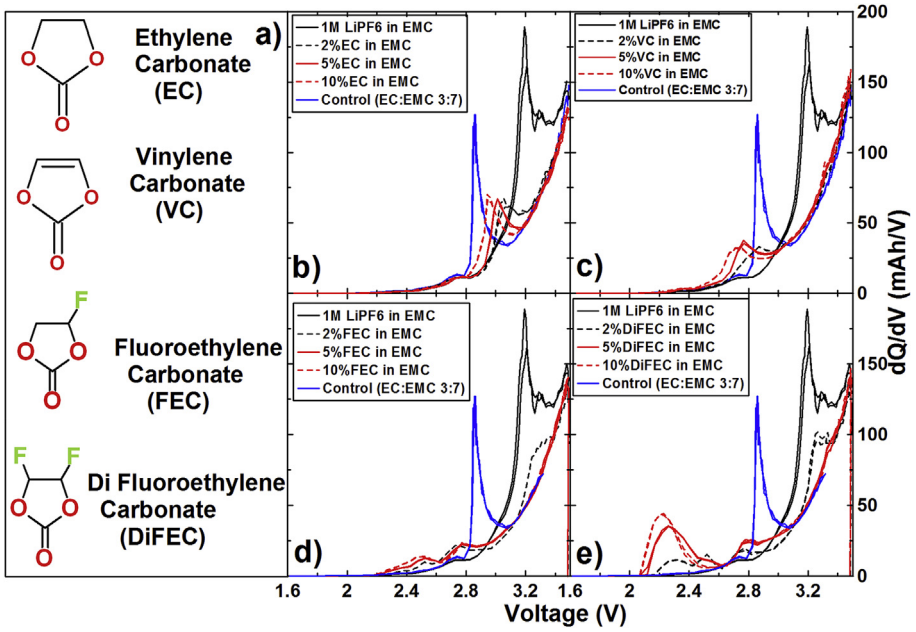

Fig. 1. a) Chemical structure of the four enablers described in this work. Differential capacity (d*Q*/d*V*) versus potential (*V*) during formation step 1 for the 180 mAh NMC442/graphite pouch cells with different enabler concentration: b) EC, c) VC, d) FEC and e) DiFEC.

Table 1
List of abbreviations, additives and their ability to passivate the graphite electrode when used in 1 M $LiPF_6$ in EMC (no EC).

Additives	Ability to passivate the graphite electrode
EC - ethylene carbonate	Yes
VC - vinylene carbonate	Yes
PES - prop-1-ene,1,3-sultone	Yes
FEC - fluoroethylene carbonate	Yes
DiFEC - (4R,5S)-4,5-Difluoro-1,3-dioxolan-2-one	Yes
MEC - methylene-ethylene carbonate	Yes
SA - succinic anhydride (SA)	Yes
MA - maleic anhydride	No
DPC - diphenyl carbonate	No
VEC – vinyl ethylene carbonate	No

such as vinylene carbonate (VC), fluoroethylene carbonate (FEC) or (4R,5S)-4,5-Difluoro-1,3-dioxolan-2-one (DiFEC) were added at 2, 5 or 10% levels by weight and are referred as "enablers" Fig. 1a shows the structure of these enablers. Some promising electrolyte additive blends in EC:EMC 3:7 electrolyte were choosen for comparison. These additive blends include, 2% VC, 2% prop-1-ene1,3-sultone (PES) and 2% PES + 1% ethylene sulphate (DTD) + 1% (tris trimethylsilyl phosphite) TTSPi (PES211). These additives were shown to yield NMC(111)/graphite cells with excellent cycling performance as well as enhance cycling performance to 4.4 V and 4.5 V for NMC(442)/graphite cells. Interested readers can refer to References [40] and [41]. The purities and the suppliers of the solvents and additives used are listed in Table S1 (supporting information).

2.2. Pouch cell, formation and degassing

Machine-made 180 mAh $Li[Ni_{0.4}Mn_{0.4}Co_{0.2}]O_2$ (NMC442)/graphite pouch cells were used throughout this study. The pouch cells were sealed under vacuum without electrolyte in China, then shipped to our laboratory in Canada. Fig. S3 shows a picture of one of the pouch cells as well as SEM images of the particles that make up the electrodes of the pouch cells. The 402035-size pouch cells were manufactured by Li-Fun Technology (Xinma Industry Zone, Golden Dragon Road, Tianyuan District, Zhuzhou City, Hunan Province, PRC, 412000). Cells were balanced for 4.7 V operation. The negative electrode of these cells was composed of 96% artificial graphite particles (15–30 μm), 2% carbon black and 2% carboxymethylcellulose (CMC)/styrene butadiene rubber (SBR) binder. The positive electrodes were composed of 96% $Li[Ni_{0.4}Mn_{0.4}Co_{0.2}]O_2$ (NMC442) particles (5–15 μm), 2% carbon black and 2% polyvinylidene fluoride (PVDF) binder. The NMC442 was supplied by Umicore and the artificial graphite was supplied by BTR New Materials Co.

Before filling with electrolyte, the cells were cut just below the heat seal and dried at 80 °C under vacuum for 14 h, to remove most of the residual water. Then the cells were transferred, without exposure to air, to an argon-filled glove box where they were filled with 0.75 mL (0.86 g for 1 M $LiPF_6$ in EMC or 0.90 g for 1 M $LiPF_6$ in EC:EMC 3:7) of electrolyte. After filling, cells were vacuum-sealed with a compact vacuum sealer (MSK-115A, MTI Corp.) at a gauge pressure of −90 kPa and temperature of 150. °C for 5 s.

Cells were then placed in a temperature box at 40. °C, where they were held at 1.5 V for 24 h, to allow for the completion of wetting. Cells were then charged at 9 mA (C/20) to 3.5 V. This step is called "formation step 1". After formation step 1, cells were transferred into the glove box, cut open to release any gas generated and vacuum sealed again. The NMC442/graphite cells destined for 4.5 V operation were charged to 4.5 V at C/20 and degassed a second time at 4.5 V. These degassing voltages were selected based on the in-situ gas evolution experiments, which showed that most of the gas evolves in the formation cycle at voltages below 3.5 V and above 4.3 V [42]. After the two degassing processes, cells were then discharged to 3.8 V where impedance spectra were measured.

2.3. UHPC barn-charge protocols

The "barn-charge" cycling procedure (see Fig. S4 in the supporting information) was designed so that cells were exposed to higher potentials for significant fractions of their testing time, thereby highlighting the effects of electrolyte oxidation at high voltage. Barn-charge cycling was carried out using the Ultra-High Precision Charger (UHPC) at Dalhousie University [16]. The "barn charge" protocol consisted of a C/15 charge to 4.2 V, followed by a slower, C/40 charge to 4.5 V. The cells were then discharged, using a slow, C/40 current to 4.2 V, followed by a C/15 discharge to 2.800 V. This process was repeated on the UHPC for 15 cycles where comparisons were made.

2.4. Storage protocols

2.4.1. 4.2 V storage

After formation step 1 (charge to 3.5 V), some cells were charged to 4.2 V and cycled between 4.2 V and 2.8 V twice using currents corresponding to C/20. Cells were then held at 4.2 V for 24 h. Cells were then carefully moved to the storage system which monitored their open circuit voltage every 6 h for a total storage time of 500 h [39]. Storage experiments were made at 40. ± 0.1 °C.

2.4.2. 4.5 V storage

After formation step 2 (charge to 4.5 V), cells were first discharged to 2.8 V and charged to 4.5 V twice using a C/20 current. Cells were then held at 4.5 V for 24 h. Finally, cells were carefully moved to the storage system which monitored their open circuit voltage every 6 h for a total storage time of 500 h [39]. Storage experiments were made at 40. ± 0.1 °C.

2.5. Ex-situ gas volume measurements

Ex-situ gas measurements were made by suspending pouch cells from a fine wire "hook" attached under a Shimadzu balance (AUW200D) [14]. The pouch cells were immersed in a beaker of deionized "nanopure" water (18 MΩ) at 20. ± 1 °C. Before weighing, all cells were charged or discharged to 3.80 V. The changes in the weight of the cell suspended in fluid, before, during and after testing are directly related to the volume changes by the change in the buoyant force. The change in mass (i.e. the balance reading) of a cell, Δm, suspended in a fluid of density, ρ, is related to the change in cell volume, Δv, by

$$\Delta v = -\Delta m/\rho \quad (1)$$

2.6. Electrochemical impedance spectroscopy

Electrochemical impedance spectroscopy (EIS) measurements were conducted on NMC442/graphite pouch cells after formation and after cycling on the UHPC [43]. Cells were charged or discharged to 3.80 V before they were moved to a 10. ± 0.1 °C temperature box. Electrochemical impedance spectra were collected with ten points per decade from 100 kHz to 10 mHz with a signal amplitude of 10 mV at 10. ± 0.1 °C. A Biologic VMP-3 was used to collect these data. The experimental setup did not allow for reproducible solution resistance measurements due to irreproducible cable and connector impedance. Therefore, all impedance spectra were shifted to 0 on the real axis at the highest frequency measured.

2.7. Long-term cycling

Long term0.5 °C cycling was performed using Neware battery testing stations. Cells were housed at 40. °C ± °C in a temperature controlled box. Cells were cycled between 2.8 and 4.4 V or 4.5 V using a constant current of C/2.2. A constant voltage step was added at the top of charge and applied until the current dropped below C/20.

3. Results and discussion

Fig. 1b–e shows the differential capacity (dQ/dV) vs. V curves for NMC442/graphite pouch cells with different amounts of EC, VC, FEC and DiFEC in an EMC-based electrolyte system during formation step 1 (first charge to 3.5 V). From the dQ/dV vs. V curves, one can determine at which potential additives or solvents initially react with the graphite electrode. Fig. 1b shows that cells with 1 M $LiPF_6$ in EMC have a differential capacity peak around 3.2 V (graphite electrode around 0.45 V vs. Li/Li^+) which is caused by the reduction of EMC at the graphite electrode surface. The large area under the peak indicates that the reduction of EMC leads to the formation of a poor passivating layer. This is similar to the results presented by Nie et al. in an earlier publication [44]. Fig. 1b shows that the addition of only 2% EC eliminates the peak at 3.2 V associated with the reduction of EMC. At the same time, a small peak near 3.05 V (graphite around 0.8 V vs. Li/Li^+) appears with a much smaller area. This peak is associated with the well-known EC reduction at the graphite electrode surface [45–56]. The small area under this peak indicates that the reduction of EC leads to the formation of a passivating layer that prevents EMC reduction. Fig. 1b shows that increasing EC loading from 2% to 30% (control), causes the dQ/dV peak to shift from 2.9 V to 2.85 V (graphite around 0.75 V vs. Li/Li^+).

Fig. 1c shows that when 2% VC was added to the EMC electrolyte system, the reduction of EMC is eliminated. This is evidenced by the disappearance of the dQ/dV peak around 3.2 V and the appearance of a small peak around 2.5 V. The peak around 2.5 V can be associated with the reduction of VC and the subsequent graphite passivation as shown by Petibon and Xia et al. [33]. Increasing the VC loading from 2% to 10% causes the reduction peak to shift from 2.9 V (0.75 V vs. Li/Li^+) to 2.7 V (graphite around 1.0 V vs. Li/Li^+).

Fig. 1d also shows that the addition of 2% FEC to EMC electrolyte leads to the partial suppression of the peak associated with the reduction of EMC. The addition of 2% FEC also leads to the appearance of two peaks around 2.5 V and 2.8 V. These peaks are associated with the reduction of FEC and subsequent partial graphite electrode passivation. The fact that the peak associated with the reduction of EMC is not totally suppressed with the addition of 2% FEC indicates that the enabler loading is too low to create a satisfactory passivating layer. This is evidenced by the fact that the addition of 5% FEC or 10% FEC leads to the total suppression of the peak associated with the reduction of EMC.

Fig. 1e shows that the case of DiFEC is very similar to the case of FEC. That is, the addition of 2% DiFEC leads to the partial suppression of the peak associated with the reduction of EMC and the appearance of a new peak around 2.2 V (graphite around 1.45 V). Further increasing the initial DiFEC loading to 5% or 10% totally suppresses the peak associated with the reduction of EMC.

In general, Fig. 1 indicates that small loadings of EC, VC, FEC and DiFEC can enable the use of EMC as sole solvent. Fig. 1 also shows that the initial loading of these enablers needed to passivate the graphite surface differs from one compound to the next. For instance while 2% EC or VC seems sufficient, an initial loading greater than 2% is needed if FEC or DiFEC are to be used.

Fig. 2 shows typical data collected during some of the experiments performed. Two electrolyte systems including control (1 M $LiPF_6$ in EC:EMC 3:7) and 2% VC in 1 M $LiPF_6$ EMC electrolyte were selected for illustrative purposes. Fig. 2a shows the coulombic efficiency (CE) versus cycle number for the two electrolyte systems during the barn-charge protocol to 4.5 V on the UHPC chargers. The coulombic inefficiency (CIE = 1 − CE) values used for comparative purposes in the next Figures were calculated from the CE taken as an average of the final three data points (cycles 13–15) collected on the UHPC. Smaller values of CIE mean the cells had higher CE and should have longer cycle and calendar life as shown by Burns et al. [2] and Wang et al. [57]. For instance, Fig. 2a shows that cells containing 2% VC in EMC electrolyte have much lower CIE than cells containing control electrolyte. Cells containing 2% VC in EMC are then expected to have longer lifetime than cells with an EC:EMC electrolyte without additives.

Fig. 2b shows the charge endpoint capacity (mAh) versus cycle number for these two electrolyte systems during the barn-charge protocol on the UHPC. The charge endpoint capacity slippage rate (mAh/cycle) values used to compare various electrolyte blends in the next Figures were calculated from the slope of a best fit line to the final five points (cycles 11–15) of the charge endpoint capacity versus cycle number curves. Charge endpoint capacity slippage is caused by undesired reactions such as electrolyte oxidation or transition metal dissolution at the positive electrode [58]. High solvent oxidation rate ultimately leads to electrolyte depletion and cell failure. Lower electrolyte oxidation rate then generally leads to cells with longer life-time as shown by Burns et al. [2]. For instance, Fig. 2b shows that cells containing 2% VC in EMC electrolyte have smaller charge endpoint capacity slippage (less electrolyte oxidation) than cells containing control electrolyte. Once again cells with the 2% VC in EMC electrolyte are expected to have a longer lifetime than the cells with the EC:EMC electrolyte without additives.

Fig. 2c shows typical open circuit voltage (OCV) versus time during 500 h storage at 40. ± 0.1 °C for NMC442/graphite cells with the two electrolyte systems. The voltage drop (V_{drop}) during storage indicates the occurrence of electrolyte oxidation at the positive electrode and has been shown to correlate well with charge endpoint capacity slippage [58]. That is, cells with large charge endpoint capacity slippage during cycling normally have large voltage drops during storage. Fig. 2c shows cells containing 2% VC in EMC electrolyte have smaller V_{drop} (less electrolyte oxidation) than cells containing control electrolyte which agrees well with Fig. 2b.

Fig. 2d shows the capacity versus cycle number for the NMC442/graphite pouch cells containing the two electrolytes during long-term cycling. These cells were cycled between 2.8 V and 4.4 V at 40. ± 0.5 °C using currents corresponding to C/2.3 (80 mA). A constant voltage step was added at the top of charge and applied until the current dropped below C/20. Fig. 2d shows cells containing 2% VC in EMC electrolyte have better capacity retention than cells containing control which agrees well with the data in

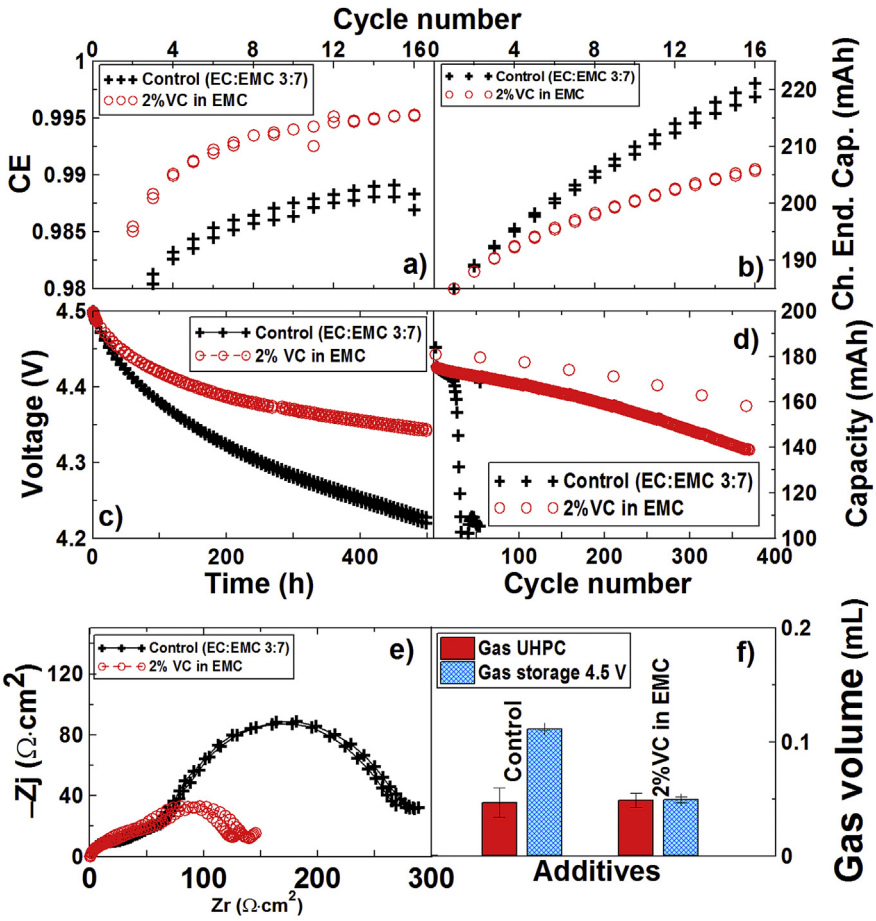

Fig. 2. a) Coulombic efficiency *vs.* cycle number during barn-charge cycling protocol on the UHPC (2.8–4.5 V, 40. °C, see Fig. S4); b) Charge endpoint capacity *vs.* cycle number during the barn-charge cycling protocol on the UHPC; c) Open circuit voltage versus time during 500 h storage at 40. °C; d) capacity vs cycle number during long-term cycling between 2.8 V and 4.4 V at 40. °C and with currents corresponding to C/2.2; e) Nyquist plots after UHPC cycling and f) Gas evolution after UHPC cycling for NMC442/graphite pouch cells with electrolytes as indicated. Fig. 2 gives example data showing the methods used in this paper.

Fig. 2a, b and c.

Fig. 2e shows the impedance spectra for the NMC442/graphite pouch cells containing the two electrolytes measured after UHPC cycling. The EIS measurements were made at 10. °C with a cell voltage of 3.80 V. The total diameter of the overlapping semicircles represents the sum of the charge-transfer resistances at both the positive and negative electrodes plus the desolvation energy of Li^+ and the charge transfer resistance from the current collector to the active material. In this work, the sum of these contributions is referred to as R_{ct} [59–62]. R_{ct} was calculated from the width of the semi-circle in the Nyquist representation of the electrochemical impedance spectra. Smaller values of R_{ct} as well as small increases in R_{ct} are desired for cells cycled for the same period of time. Fig. 2e shows that cells containing 2% VC in EMC electrolyte have smaller R_{ct} than cells containing control electrolyte.

Fig. 2f shows the gas evolution for the NMC442/graphite pouch cells containing the two different electrolytes after storage at 4.5 V at 40. °C (500 h) and after UHPC cycling at 40. °C to 4.5 V. Smaller values of gas evolution are desired for cells cycled during the same period of time. The initial volume of the pouch cells was 2.2 mL. A volume change during cycling less than 10% (0.22 mL) is desired in order to prevent pressure build up in hard-can cell designs and loss of stack pressure in cell designs with soft enclosures. Fig. 2f shows cells containing 2% VC in EMC electrolyte produce a similar amount of gas to cells containing control during UHPC cycling. Fig. 2f shows cells containing 2% VC in EMC electrolyte produce less gas than cells containing control electrolyte during storage at 4.5 V and 40. °C. However, all cells have do not have a gassing problem (gas volume < 0.22 mL) during the cycling or storage processes evaluated here.

Fig. 3 summarizes the cycling data collected on the UHPC including CIE, discharge capacity fade rate, charge endpoint capacity slippage and the increase in ΔV/cycle for NMC442/graphite cells with different electrolytes tested at 40. ± 0.1 °C using the barn-charge protocol (see Fig. S4) to 4.5 V. The detailed data for CE, discharge capacity, charge endpoint capacity and ΔV, all plotted vs cycle number are given in Figs. S5, S6, S7 and S8 in the supporting information. The discharge capacity fade rate, charge endpoint capacity slippage and the increase in ΔV/cycle were calculated from the slope of a best fit line to the final five points (cycles 11–15) of the data given in Figs. S5, S6, S7 and S8. Each data point in Fig. 3 represents the average of two cells, and the error bars are the standard deviation of the results. Fig. 3 shows that adding VC to control (EC:EMC) electrolyte increases CIE (bad) while adding PES or PES 211 decreases CIE (good) during the barn-charge protocol to 4.5 V. This is consistent with publications that show adding PES or PES211 improves capacity retention, decreases impedance growth and decreases gas evolution during high voltage cycling [41,63].

Fig. 3 shows that cells containing 1 M $LiPF_6$ in EMC electrolyte without enablers have lower CIE, lower fade rate and lower charge endpoint capacity slippage than cells containing control electrolyte. Fig. 3 clearly shows the benefit of reducing amount of EC in the EMC

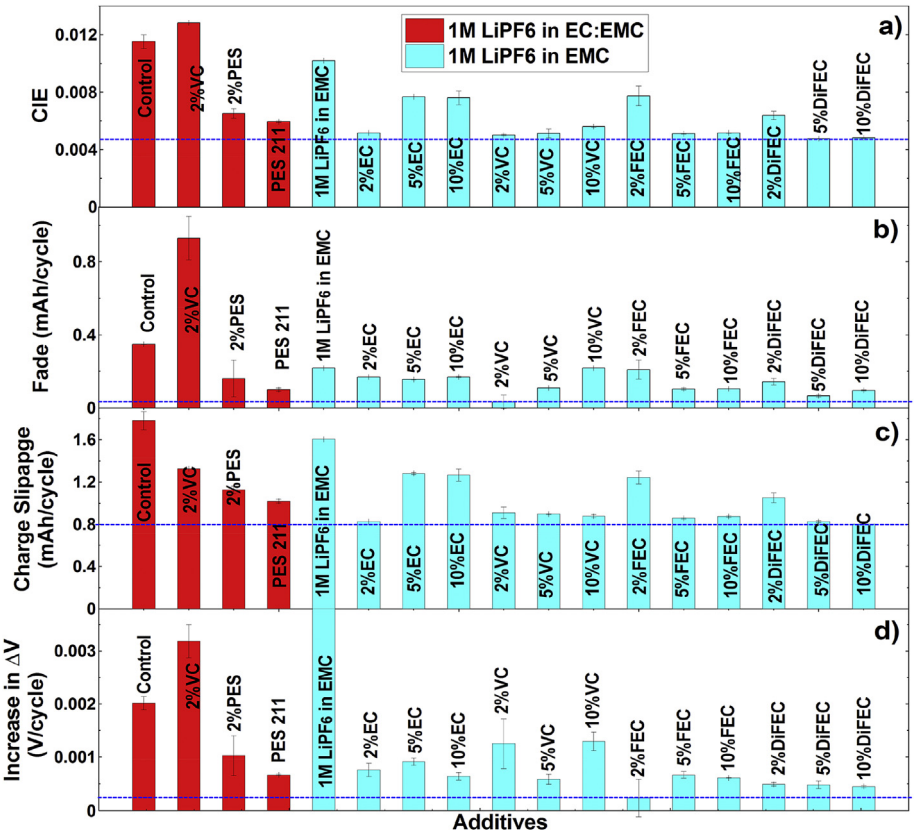

Fig. 3. Summary of cycling data collected on the UHPC:a) CIE (CIE = 1 − CE), b) fade rate, c) charge endpoint capacity slippage and d) ΔV for NMC442/graphite pouch cells cycled to 4.5 V at 40. °C using the barn-charge protocol shown in Fig. S4.

electrolyte. For instance, Fig. 3 shows that electrolytes consisting of 1 M $LiPF_6$ EC:EMC, where the EC content is less than 30%, provide far superior cycling performance than cells with a 1 M $LiPF_6$ EC:EMC (3:7) electrolyte. Fig. 3 also shows that there is an optimum EC loading. For instance, CIE, charge endpoint capacity slippage rate, fade rate and polarization growth rate improve going from pure EMC to EC:EMC (2:98) and then worsen going from EC:EMC (2:98) to EC:EMC (10:90). The improvement upon addition of 2% EC to pure EMC probably comes from a better passivation of the graphite surface. The performance decline following the increase of EC loading can be associated with larger amount of left-over EC following the passivation of the graphite surface. It is likely that the EC left over following the passivation of the negative electrode is oxidized at the positive electrode during the 4.5 V b protocol which leads to poorer cycling performance.

Similarly to the case of EC, Fig. 3 also shows that there is an optimum VC loading. For instance, Fig. 3 shows that adding 2% VC to EMC improves cell performance while increasing VC loading to 5% or 10% worsens cell performance when cycled to high voltage compared to cells containing 2% VC. Petibon, Xia et al. [33] showed that the VC loading needs to be optimized in EMC-based electrolyte. They showed that the initial amount of VC added to the electrolyte needs to be large enough to provide good graphite passivation while kept low enough to minimize the amount of VC remaining in the electrolyte that can be oxidized. Petibon, Xia et al. [33] showed that an optimized VC loading in EMC-based electrolyte led to NMC(442)/graphite cells cycled to both 4.4 V and 4.5 V having low gas generation during formation and cycling, low impedance, low charge slippage rate as well as low CIE.

Fig. 3 also shows that the results for FEC and DiFEC are very similar those for EC and VC. However, Fig. 3 shows that lower loadings (such as 2%) of FEC or DiFEC are not sufficient to fully passivate the graphite as evidenced by a high CIE and a high charge endpoint capacity slippage. However, 5% FEC or 5% DiFEC lead to good cell performance, better than the EC-based electrolyte with the optimized additive blend. Fig. 3 also shows that increasing FEC or DiFEC loading to 10% does not improve the performance compared to an initial loading of only 5%.

Fig. 4a summarizes V_{drop} during 500 h storage at 4.2 V (red color) and 4.5 V (cyan color). All storage data were collected at 40. ± 0.1 °C. Detailed storage data are given in Figs. S9 and S10. Smaller V_{drop} means cells have less electrolyte oxidation at the positive electrode during storage [39]. Fig. 4a shows that adding VC, PES or PES 211 in EC:EMC electrolyte decreases V_{drop} at both 4.2 V and 4.5 V compared to control electrolyte similarly to the data in References 50 and 58. Fig. 4a shows adding EC (2%–30%) to EMC electrolyte does not obviously impact V_{drop} at both 4.2 V and 4.5 V Fig. 4a shows adding 2% VC to EMC electrolyte greatly decreases V_{drop} at both 4.2 V and 4.5 V compared to both pure EMC electrolyte and EC:EMC electrolytes with various additive blends. Increasing the initial VC loading from 2% to 5% or 10% does not impact V_{drop} at 4.2 V, however it increases the V_{drop} at 4.5 V when 10% VC was used. This again suggests that there is an optimal VC loading as suggested by Petibon, Xia et al. [33] and in Fig. 3.

Fig. 4a shows that loadings of 2% FEC or 2% DiFEC are too low since V_{drop} is still large. However, increasing the FEC or DiFEC content to 5% reduces V_{drop} to the same order as V_{drop} for cells with EMC:VC (98:2) electrolyte. Further increasing the initial FEC or DiFEC loading to 10% did not change V_{drop} compared to the results for cells with 5% FEC or 5% DiFEC. These results agree well with the

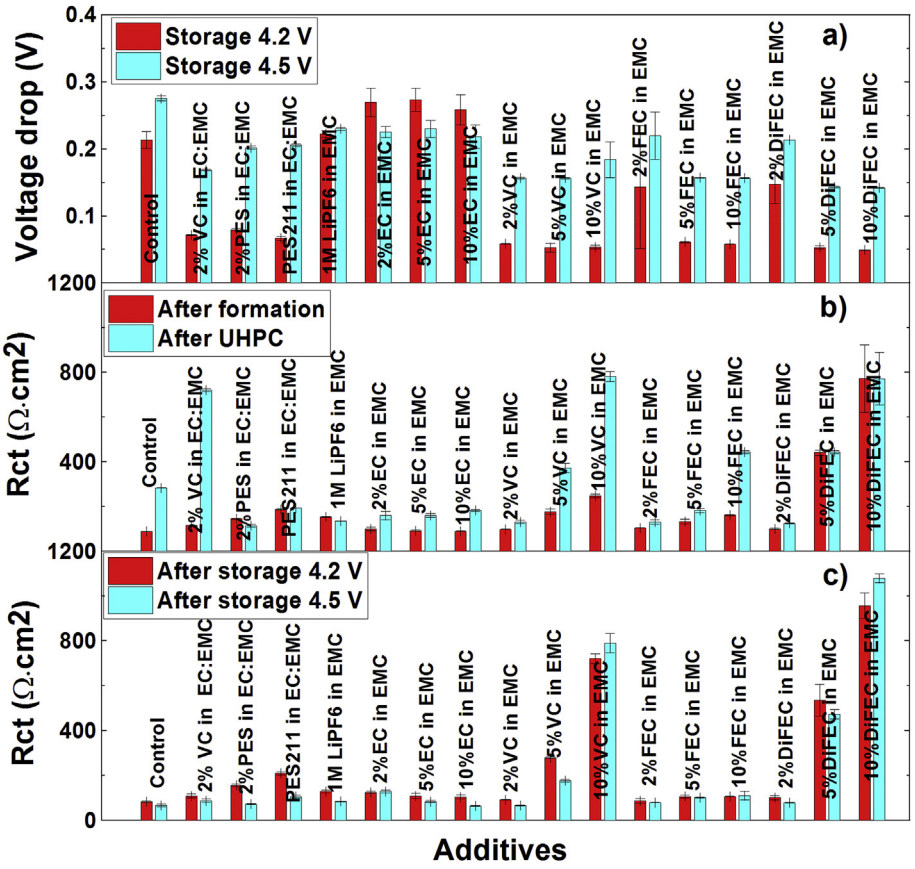

Fig. 4. a) Summary of a) V_{drop} during 500 h storage at 4.2 V (red bars) or 4.5 V (cyan bars); b) Summary of the charge transfer resistance (R_{ct}) measured after formation (red bars) and after UHPC cycling (cyan bars); c) Summary of the charge transfer resistance (R_{ct}) measured after 500 h storage at 4.2 V (red bars) and after 500 h storage at 4.5 V (cyan bars). (For interpretation of the references to color in this figure legend, the reader is referred to the web version of this article.)

charge endpoint capacity slippage data in Fig. 3c. Generally, Fig. 4a shows that FEC, VC and DiFEC are much superior to EC when used as enablers in EMC-based electrolytes. Fig. 4a also shows that NMC(442)/graphite cells filled with an EMC-based electrolyte having optimized VC, FEC or DiFEC content have a lower electrolyte oxidation rate than cells filled with an EC-based electrolyte with an effective ternary additive blend. This is similar to the data presented by Petibon, Xia et al. [33]. Fig. 4 also further supports the idea that excess EC in the electrolyte leads to a larger electrolyte oxidation rate.

Fig. 4b shows a summary of the magnitude of the impedance (R_{ct}) after formation (red color) and after 600 h of UHPC cycling (cyan color). Detailed EIS spectra for all of the cells tested after formation and after UHPC cycling are given in Figs. S11 and S12, respectively. All the EIS measurements were made at 3.80 V and at 10. ± 0.1 °C. Fig. 4b clearly shows that the problem of using VC in EC:EMC electrolyte since the impedance increases a lot after UHPC cycling while the benefit of using PES or PES 211 in EC:EMC electrolyte is mainly in impedance control during cycling. Fig. 4b shows adding 2% VC, 2% FEC or 2% DiFEC to EMC electrolyte leads to cells with smaller impedance than cells containing 2% VC in 1 M $LiPF_6$ EC:EMC 3:7 and cells with PES211 electrolyte. Increasing the initial VC, FEC or DiFEC content past 2% leads to an increase of cell impedance after formation and UHPC cycling. The impedances of cells containing 10% of these enablers are simply too high to be useful. This further shows the importance of optimizing the initial enabler loading.

Fig. 4c shows a summary of the EIS data after storage at 4.2 V (red color) and after storage at 4.5 V (cyan color). Detailed EIS spectra for all of the cells tested after storage at 4.2 V and after storage at 4.5 V are given in Figs. S13 and S14, respectively. Fig. 4c shows that adding VC, PES or PES 211 in control electrolyte yields cells with higher impedance at 4.2 V but similar impedance at 4.5 V Fig. 4c shows that increasing the amounts of EC or FEC from 2% to 10% in EMC electrolyte does not obviously impact the impedance after storage at both 4.2 V and 4.5 V Fig. 4c shows that adding a high level of VC or DiFEC to EMC electrolyte greatly increases the impedance after storage at both 4.2 V and 4.5 V. These trends are similar to the impedance data after formation or UHPC cycling in Fig. 4b.

Fig. 5a shows the volume of gas produced during formation step 1 (charge to 3.5 V) and formation step 2 (charge to 4.5 V), respectively. The gas created during formation step 1 is caused by the passivation of graphite on the negative electrode while the gas during formation step 2 is caused by electrolyte oxidation and the passivation of the NMC electrode when the electrode is first charged to 4.5 V [42]. Fig. 5a shows that cells containing control electrolyte produced 1.3 mL gas during formation step 1 and 0.2 mL gas during formation step 2, respectively. The large amount of gas (mostly ethylene) generated during the first formation step in cells containing the control electrolyte comes from the reduction of EC. Adding VC, PES or PES 211 to EC:EMC electrolyte greatly decreased the amount of gas produced during formation step 1 due to the reduction of the additives which lead to few gaseous by-products. Cells containing VC in EMC electrolyte produced more gas at higher VC loading during formation step 2 due to the instability of VC at high voltages [41].

Fig. 5a shows that cells containing 1 M $LiPF_6$ in EMC electrolyte

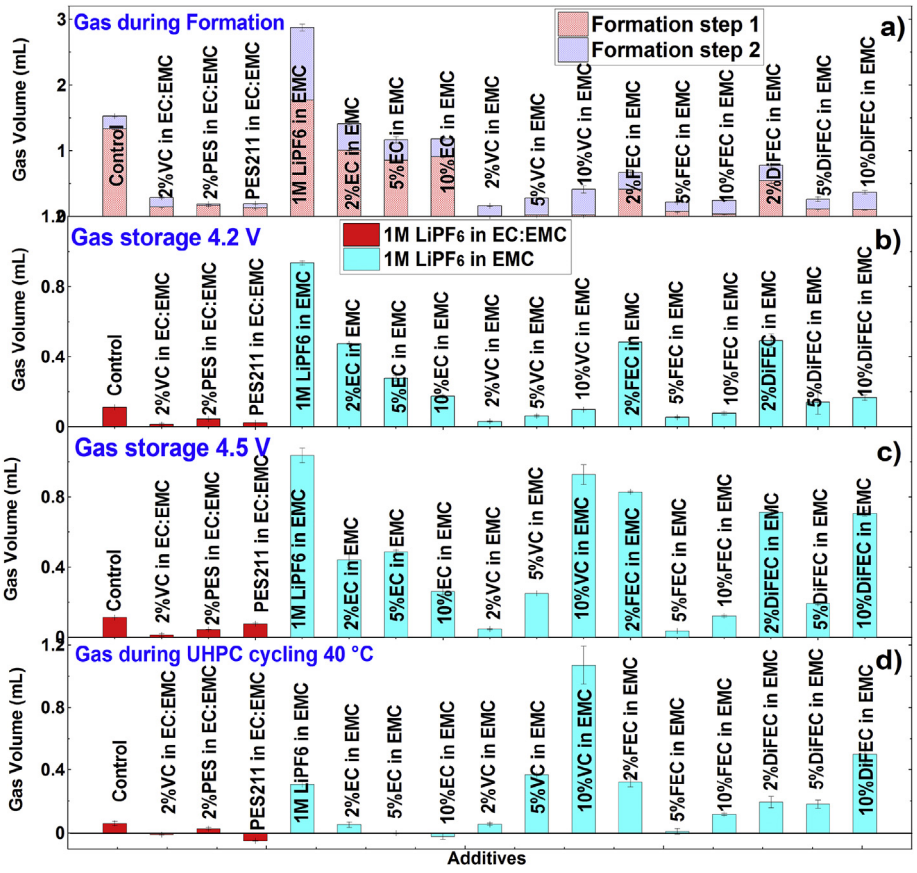

Fig. 5. Summary of the gas evolution during: a) formation; b) 500 h storage at 4.2 V and 40. °C; c) 500 h storage at 4.5 V and 40. °C and d) UHPC cycling (2.8–4.5 V, 40. °C, protocol shown in Fig. S4).

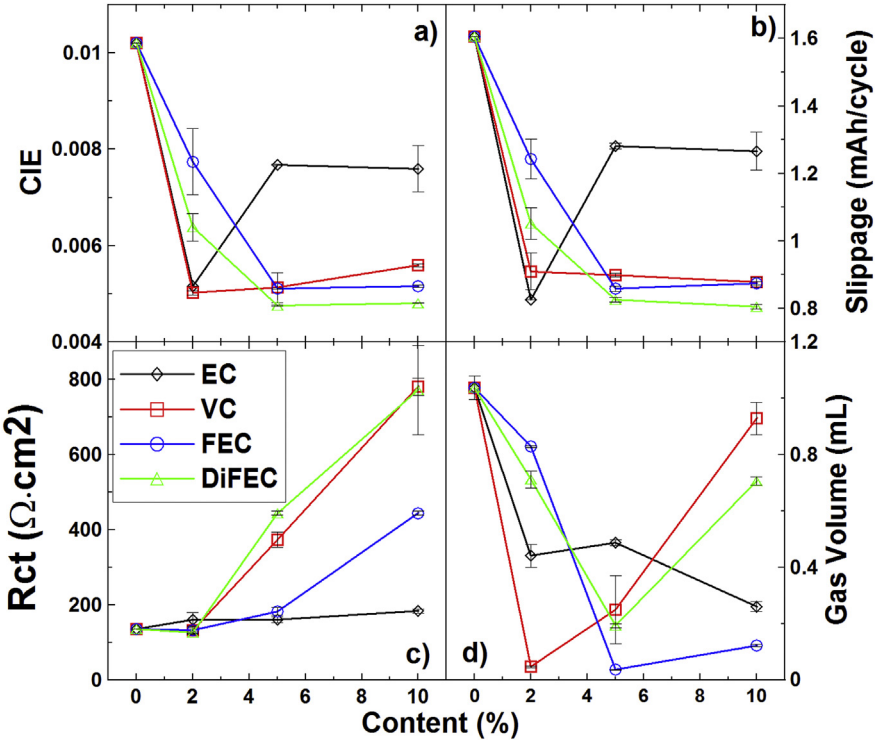

Fig. 6. Summary of: a) CIE; b) charge endpoint capacity slippage; c) R_{ct} and d) gas evolution, all plotted as a function of additive content during UHPC cycling (2.8–4.5 V, 40. °C, protocol shown in Fig. S4).

produced a large amount of gas during both formation step 1 and formation step 2 due to the poor passivation of graphite electrode. Fig. 5a shows that adding EC to EMC electrolyte decreases the gas evolution during both formation step 1 and step 2. However, the amounts of gas produced by cells with EMC-EC electrolyte are still large during formation step 1 due the reduction of EC which leads to the production of gaseous by-products [64].

Fig. 5a shows that adding only 2% VC to EMC electrolyte virtually eliminates the gas evolution during formation step 1 while the adding 2% FEC or 2% DiFEC is obviously not enough since the gas production is still large. Higher concentrations of VC, FEC or DiFEC decrease gas production during formation step 1, but slightly increase gas evolution during formation step 2. Again, the concentration of the enablers need to be optimized in order to minimize gas production during formation.

Fig. 5b–d shows a summary of gas evolution data during 500 h storage at 4.2 V and 40. °C, 500 h storage at 4.5 V and 40. °C, and 600 h UHPC cycling at 40. °C, respectively. Fig. 5b–d shows that adding VC, PES or PES 211 to control electrolyte greatly decreases the gas evolution during cycling or storage experiments. This again is one of the advantages of the addition of such additive blends in EC-based electrolytes used in NMC(442)/graphite cells cycled to high voltage as shown by Xia et al. [63].

Fig. 5b–d shows that cells containing 1 M $LiPF_6$ in EMC electrolyte have a large amount of gas evolution during both storage and cycling experiments. This probably is caused by the poor graphite passivation. Fig. 5b–d shows that adding EC to EMC electrolyte decreases gas evolution. However, gas evolution for these EC-containing cells without additives is still high during the storage experiments. Fig. 5b–d shows that adding 2% VC to EMC greatly decreases the gas evolution during storage at 4.2 V, 4.5 V and cycling to 4.5 V. However, increasing the initial VC loading to 5% or 10%, leads to large gas evolution caused by oxidation at the positive electrode of excess VC remaining in the electrolyte after formation [33].

Fig. 5b–d shows that cells with 2% FEC or 2% DiFEC in EMC-based electrolyte produced large amounts of gas during storage and UHPC cycling tests due to improper graphite passivation. When the amount of FEC or DiFEC was increased to 5%, the gas evolution decreased during cycling or storage to acceptable values. However further increasing the FEC or DiFEC content to 10% leads to an increase in gas production. This once again shows the importance of optimizing the enabler loading.

Fig. 6 summarizes the CIE, charge slippage, R_{ct} and gas evolution as a function of additive content during UHPC cycling. Fig. 6 shows that only VC can function well at the 2% level in EMC, while EC, FEC or DiFEC are not effective at the 2% level. Fig. 6 shows that cells with 5% VC, FEC or DiFEC in EMC all have low CIE and low charge endpoint capacity slippage. However, only cells containing 5% FEC have low impedance after cycling and storage tests. If the content of

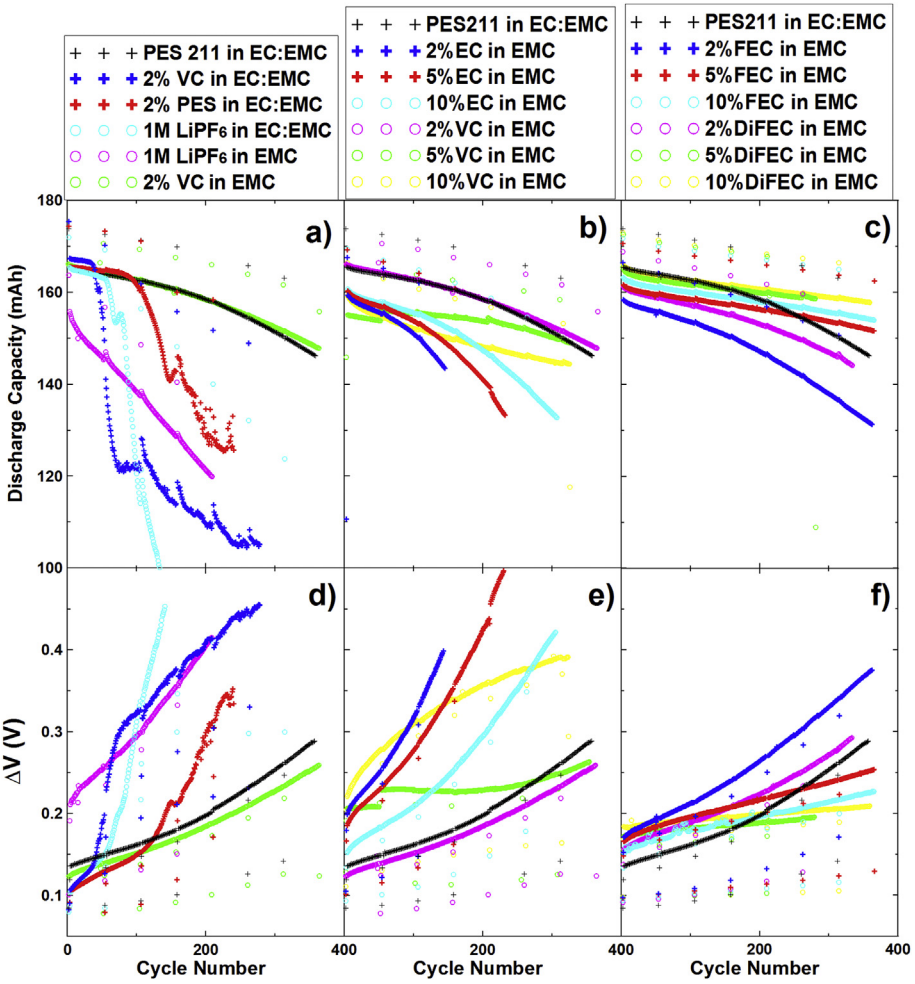

Fig. 7. a, b, c) Discharge capacity and d, e, f) ΔV, all plotted vs. cycle number for NMC442/graphite pouch cells containing different electrolytes as indicated. "Control" designates cells with 1 M $LiPF_6$ in EC:EMC 3:7. The cycling was between 2.8 and 4.4 V at C/2.1 (80 mA) at 40. ± 0.5°C using CCCV protocol.

these enablers is increased to 10%, then the CIE and slippage remain the same while the impedance and gas evolution increase significantly. Fig. 6 suggests that the optimum amount of VC is near 2% while the optimum amount of FEC and DiFEC is between 2% and 5%.

Figs. 7 and 8 show the long-term cycling data (capacity retention and ΔV) for NMC442/graphite cells with all the electrolyte blends cycled to 4.4 V and 4.5 V, respectively. The long-term cycling cells were the same cells used for the UHPC cycling experiments and the long-term cycling began immediately after the UHPC cycling completed. All cells in Figs. 7 and 8 were cycled at 40. ± 0.5 °C using currents corresponding to about C/2.2 (80 mA). Figs. 7 and 8 show that cells containing PES 211 in EC:EMC electrolyte performed much better than cells containing control, 2% VC or 2% PES in EC:EMC electrolyte confirming the superiority of the ternary additive blend in NMC(442)/graphite cells containing an EC-based electrolyte and cycled to high voltage [15,41]. Fig. 7 shows that all cells containing EC as an enabler in EMC electrolyte perform worse than PES211 in EC:EMC electrolyte at 4.4 V. At 4.5 V, cells containing EC as an enabler in EMC electrolyte perform similarly to cells containing PES211 in EC:EMC electrolyte. Ma et al. [41] showed that the impact of additives in EC:EMC-based electrolytes became insignificant as NMC/graphite cells were charged and discharged repeatedly above 4.5 V at C/10. The results here are consistent with Ma's results.

Fig. 7 shows that cells containing 2% VC in EMC electrolyte have slightly better capacity retention than cells containing PES211 in EC:EMC electrolyte cycled up to 4.4 V. However, cells containing 2% VC in EMC electrolyte perform much better than PES211 at 4.5 V (see Fig. 8). This is similar to the data presented by Petibon, Xia et al. [33]. This is very encouraging since a simple electrolyte consisting of only EMC and VC performs as well at 4.4 V and better at 4.5 V than an electrolyte consisting of 5 different components (2 solvents and 3 additives). Figs. 7 and 8 show that adding large amounts of VC to EMC decreases the discharge capacity and increases ΔV during cycling due increased impedance associated with high VC content. Fig. 7 shows cells containing 2% FEC or 2% DiFEC in EMC electrolyte perform worse than cells containing PES211 in EC:EMC electrolyte at 4.4 V. Figs. 7shows that higher concentrations of FEC or DiFEC, for example 5%, can yield cells with better cycling performance than cells containing PES211 in EC:EMC electrolyte at 4.4 V. Fig. 8 shows that cells containing FEC and DiFEC as enablers in EMC electrolyte all perform better than PES 211 in EC:EMC electrolyte at 4.5 V.

Fig. S15 shows a summary of % capacity loss at cycle 350. Fig. S15 shows that many electrolyte blends in this study (EMC:VC 98:2, EMC:VC 95:5, EMC:VC 90:10, EMC:FEC 95:5, EMC:FEC 95:10, EMC:DiFEC 95:5, EMC:DiFEC 90:10) have less than 10% capacity loss during the first 350 cycles to 4.4 V using a CCCV protocol at 40. °C, which is quite impressive. For instance, cells containing EMC:DiFEC 90:10 electrolyte have only 4.7% and 13.6% capacity loss during the first 350 cycles using CCCV protocols cycled to 4.4 V and 4.5 V,

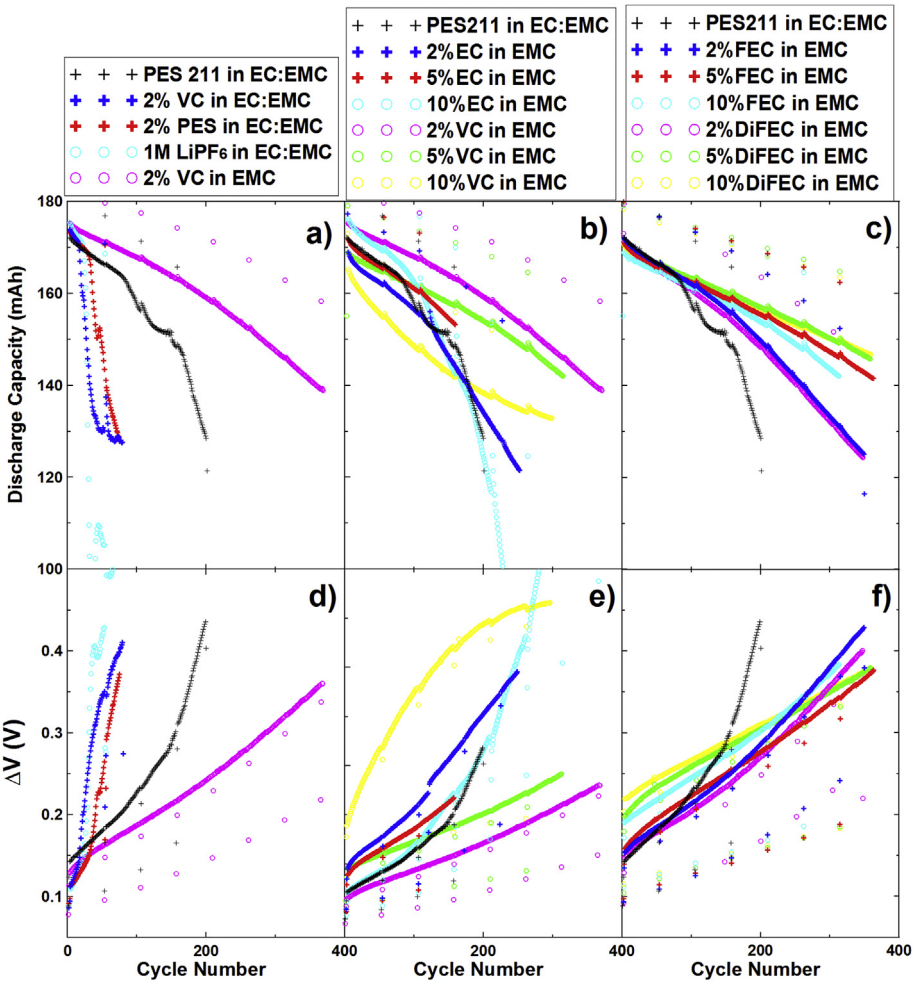

Fig. 8. a, b, c) Discharge capacity and d, e, f) ΔV, all plotted vs. cycle number for NMC442/graphite pouch cells containing different additive blends as indicated. The cycling was between 2.8 and 4.5 V at C/2.2 (80 mA) at 40. ± 0.5 °C using CCCV protocol.

respectively. Figs. 7 and 8 and Fig. S15 seem to indicate that FEC and DiFEC are superior enablers than VC. However, intermediate VC loadings between 2% and 5% must be tested in order to confirm this assertion.

Figs. S16a and S16b show a summary of the volume change and EIS data collected after the long-term cycling experiments of the same cells shown in Figs. 7 and 8. Fig. S16 shows that the failure mechanism of cells containing control, 2% VC, and 2% PES in EC:EMC electrolyte is due to the impedance growth, rather than gas evolution. Fig. S16 shows that cells containing EMC electrolyte cycled to 4.5 V have more gas generation and higher impedance than cells cycled to 4.4 V. Increasing the concentration of the enablers generally leads to higher impedance and more gas evolution as well. The above results again show the importance of optimizing the enabler loading.

Some concerns about the linear carbonate electrolyte are the volatility, the solubility of salts and the conductivity of electrolytes without EC. Fig. S17a shows the electrolyte mass lost in vacuum at room temperature for 1 M $LiPF_6$ in EC:EMC and 1 M $LiPF_6$ in EMC electrolyte, respectively. The experiment was performed with 6 mL of electrolyte placed in a vial which was placed in a small chamber which could be evacuated. The pressure reached was about −95 kPa gauge pressure during these tests. The key finding of this experiment is that the mass losses from the EC-containing and EC-free electrolytes are about the same. Both electrolytes have less than 2% mass loss during the entire test (7 min). This could be further illustrated by the vacuum sealing process where less than 0.015 g (1.7 wt%) of electrolyte loss from the pouch cells during the vacuum sealing at −90 kPa for about 20 s was observed.

Fig. S17b shows the conductivity measured as a function of the concentration of $LiPF_6$ in EMC at different temperatures. Fig. S17b shows the solubility of $LiPF_6$ in EMC is more than 2.5 M at room temperature. Fig. S17b shows that lower concentrations of $LiPF_6$ in EMC (less than 0.5 M) have very low conductivity. Fig. S17b shows the optimal amount of $LiPF_6$ in EMC is around 1.5 M, especially at low temperatures. Fig. S17b also indicates that it will be important to investigate the impact of enablers or additives with 1.5 M $LiPF_6$ in EMC electrolyte.

4. Summary and conclusions

Electrolyte systems containing EC were initially designed for Li-ion cells operated below 4.2 V. Electrolytes containing EC have been “tweaked’ over the years by using additives and co-solvents to allow for high voltage operation. The work in this paper suggests that EC itself is the root cause of many issues associated with the operation of NMC/graphite cells to high potential. Electrolyte oxidation reactions at high voltages cause gas evolution and impedance growth, leading to cell failure. These parasitic reactions become very problematic at 4.5 V even with state of the art electrolyte additives PES211 in EC:EMC electrolyte (see Fig. 8).

This work demonstrates that cyclic carbonates such as VC, FEC and DiFEC can act as the enablers for EMC-based electrolytes which function well in NMC442/graphite cells tested up to 4.4 or 4.5 V. These additives enable excellent passivation of the graphite electrode during formation. When the amount of these enablers used in the cell is too large, the excess enabler will be oxidized at high potentials, leading to gas generation and/or impedance growth. With an optimized enabler content, EMC-based electrolyte provides excellent cycling performance, low gas evolution and relatively stable impedance during cycling to 4.4 V or 4.5 V.

Further work should be done to optimize the amount of these and other enablers and to find other co-additives that can be used together with these enablers to improve cell performance. It is very likely that other enablers can also function well. It is also very likely other linear carbonates besides EMC can function well in electrolytes without EC. Further work may also include the exploration of cycling performance at high temperature, low temperature, high rate as well as the performance in different cell chemistries (ie. $LiCoO_2$ (LCO)/graphite and $LiNi_{0.80}Co_{0.15}Al_{0.05}O_2$ (NCA)/graphite Li-ion cells). It is essential that other researchers get involved in such searches.

Acknowledgments

The authors acknowledge the financial support of NSERC and 3M Canada under the auspices of the Industrial Research Chairs program. The authors thank Dr. Jing Li of BASF for providing the most of the solvents and salts used in this work. The authors thank Xiaodong Cao from HSC Corp. for providing the DiFEC. R. Petibon thanks NSERC, and the Walter C. Sumner Foundation for scholarship support.

Appendix A. Supplementary data

Supplementary data related to this article can be found at http://dx.doi.org/10.1016/j.jpowsour.2016.08.015.

References

[1] V. Etacheri, R. Marom, R. Elazari, G. Salitra, D. Aurbach, Energy Environ. Sci. 4 (2011) 3243.
[2] J.C. Burns, A. Kassam, N.N. Sinha, L.E. Downie, L. Solnickova, B.M. Way, J.R. Dahn, J. Electrochem. Soc. 160 (2013) A1451.
[3] G.G. Amatucci, C.N. Schmutz, A. Blyr, C. Sigala, A.S. Gozdz, D. Larcher, J.M. Tarascon, J. Power Sources 69 (1997) 11.
[4] Z. Lu, D.D. MacNeil, J.R. Dahn, Electrochem. Solid-State Lett. 4 (2001) A200.
[5] K.M. Abraham, D. Peramunage, US Patent, US5766796 A (1998).
[6] Y. Wang, J. Jiang, J.R. Dahn, Electrochem. Commun. 9 (2007) 2534.
[7] T. Ohzuku, R.J. Brodd, J. Power Sources 174 (2007) 449.
[8] A.K. Padhi, K.S. Nanjundaswamy, J.B. Goodenough, J. Electrochem. Soc. 144 (1997) 1188.
[9] V. Etacheri, R. Marom, R. Elazari, G. Salitra, D. Aurbach, Energy Environ. Sci. 4 (2011) 3243.
[10] M.N. Obrovac, V.L. Chevrier, Chem. Rev. 114 (2014) 11444.
[11] B. Simon, J.P. Boeuve, US Patent, US 5626981 A (1997).
[12] J.N. Reimers, B.M. Way, US Patent, US6074777 A.
[13] R.P. Day, J. Xia, R. Petibon, J. Rucska, H. Wang, A.T.B. Wright, J.R. Dahn, J. Electrochem. Soc. 162 (2015) A2577.
[14] C.P. Aiken, J. Xia, D.Y. Wang, D.A. Stevens, S. Trussler, J.R. Dahn, J. Electrochem. Soc. 161 (2014) A1548.
[15] K.J. Nelson, G.L. Eon, A.T.B. Wright, L. Ma, J. Xia, J.R. Dahn, J. Electrochem. Soc. 162 (2015) A1046.
[16] J. Xia, M. Nie, L. Ma, J.R. Dahn, J. Power Sources 306 (2016) 233.
[17] K. Xu, C.A. Angell, J. Electrochem. Soc. 149 (2002) A920.
[18] A. Abouimrane, I. Belharouak, K. Amine, Electrochem. Commun. 11 (2009) 1073.
[19] H.J. Santner, K.-C. Möller, J. Ivančo, M.G. Ramsey, F.P. Netzer, S. Yamaguchi, J.O. Besenhard, M. Winter, J. Power Sources 119–121 (2003) 368.
[20] Y. Abu-lebdeh, I. Davidson, J. Power Sources 189 (2009) 576.
[21] V. Borgel, E. Markevich, D. Aurbach, G. Semrau, M. Schmidt, J. Power Sources 189 (2009) 331.
[22] Y. Wang, K. Zaghib, A. Guerfi, F.F.C. Bazito, R.M. Torresi, J.R. Dahn, Electrochim. Acta 52 (2007) 6346.
[23] A. Deshpande, L. Kariyawasam, P. Dutta, S. Banerjee, J. Phys. Chem. C 117 (2013) 25343.
[24] A. Hofmann, M. Schulz, S. Indris, R. Heinzmann, T. Hanemann, Electrochim. Acta 147 (2014) 704.
[25] K.-C. Möller, T. Hodal, W.K. Appel, M. Winter, J.O. Besenhard, J. Power Sources 97–98 (2001) 595.
[26] M. Smart, B. Ratnakumar, V. Ryan-Mowrey, S. Surampudi, G.K. Prakash, J. Hu, I. Cheung, J. Power Sources 119–121 (2003) 359.
[27] K. Xu, S. Zhang, J.L. Allen, T.R. Jow, J. Electrochem. Soc. 149 (2002) A1079.
[28] Z. Zhang, L. Hu, H. Wu, W. Weng, M. Koh, P.C. Redfern, L.A. Curtiss, K. Amine, Energy Environ. Sci. 6 (2013) 1806.
[29] A. Kraytsberg, Y. Ein-eli, Adv. Energy Mater. 2 (2012) 922.
[30] M. Hu, X. Pang, Z. Zhou, J. Power Sources 237 (2013) 229.
[31] J.O. Besenhard, M. Winter, J. Yang, W. Biberacher, J. Power Sources 54 (1995) 228.
[32] D. Aurbach, K. Gamolsky, B. Markovsky, Y. Gofer, M. Schmidt, U. Heider, Electrochim. Acta 47 (2002) 1423.
[33] R. Petibon, J. Xia, L. Ma, S.L. Glazier, K.J. Nelson, J.R. Dahn, Novel electrolyte

system for high voltage Li-ion cells, as send to J. Electrochem. Soc. for publication on July 15, 2016.
[34] J. Xia, R. Petibon, A. Xiao, W.M. Lamanna, J.R. Dahn, J. Electrochem. Soc. 163 (2016) A1637.
[35] D. Chalasani, J. Li, N.M. Jackson, M. Payne, B.L. Lucht, J. Power Sources 67 (2012) 208.
[36] B. Li, M. Xu, T. Li, W. Li, S. Hu, Electrochem. Commun. 17 (2012) 92.
[37] G.B. Han, M.H. Ryou, K.Y. Cho, Y.M. Lee, Y.K. Park, J. Power Sources 195 (2010) 3709.
[38] T.M. Bond, J.C. Burns, D.A. Stevens, H.M. Dahn, J.R. Dahn, J. Electrochem. Soc. 160 (2013) A521.
[39] N.N. Sinha, A.J. Smith, J.C. Burns, G. Jain, K.W. Eberman, E. Scott, J.P. Gardner, J.R. Dahn, J. Electrochem. Soc. 158 (2011) A1194.
[40] J. Xia, L. Ma, J.R. Dahn, J. Power Sources 287 (2015) 377.
[41] L. Ma, J. Xia, J.R. Dahn, J. Electrochem. Soc. 161 (2014) A2250.
[42] C.P. Aiken, J. Self, R. Petibon, X. Xia, J.M. Paulsen, J.R. Dahn, J. Electrochem. Soc. 162 (2015) A760.
[43] R. Petibon, C.P. Aiken, N.N. Sinha, J.C. Burns, H. Ye, C.M. VanElzen, G. Jain, S. Trussler, J.R. Dahn, J. Electrochem. Soc. 160 (2013) A117.
[44] M. Nie, D. Chalasani, D.P. Abraham, Y. Chen, A. Bose, B.L. Lucht, J. Phys. Chem. C 117 (2013) 1257.
[45] J.O. Besenhard, M. Winter, J. Yang, W. Biberacher, J. Power Sources 54 (1995) 228.
[46] D. Aurbach, K. Gamolsky, B. Markovsky, Y. Gofer, M. Schmidt, U. Heider, Electrochim. Acta 47 (2002) 1423.
[47] G.V. Zhuang, K. Xu, H. Yang, T.R. Jow, P.N. Ross, J. Phys. Chem. B 109 (2005) 17567.
[48] J.C. Burns, R. Petibon, K.J. Nelson, N.N. Sinha, A. Kassam, B.M. Way, J.R. Dahn, J. Electrochem. Soc. 160 (2013) A1668.
[49] Y. Zhu, M.D. Casselman, Y. Li, A. Wei, D.P. Abraham, J. Power Sources 246 (2014) 184.
[50] J. Xia, J.E. Harlow, R. Petibon, J.C. Burns, L.P. Chen, J.R. Dahn, J. Electrochem. Soc. 161 (2014) A547.
[51] J. Xia, J. Self, L. Ma, J.R. Dahn, J. Electrochem. Soc. 162 (2015) A1424.
[52] M. Nie, J. Xia, J.R. Dahn, J. Electrochem. Soc. 162 (2015) A1186.
[53] J. Xia, L. Ma, C.P. Aiken, K.J. Nelson, L.P. Chen, J.R. Dahn, J. Electrochem. Soc. 161 (2014) A1634.
[54] R. Petibon, C.P. Aiken, L. Ma, D. Xiong, J.R. Dahn, Electrochim. Acta 154 (2015) 287.
[55] M. Nie, J. Xia, L. Ma, J.R. Dahn, J. Electrochem. Soc. 162 (2015) A2066.
[56] L. Madec, J. Xia, R. Petibon, K.J. Nelson, J.-P. Sun, I.G. Hill, J.R. Dahn, J. Phys. Chem. C 118 (2014) 29608.
[57] D.Y. Wang, J. Xia, L. Ma, K.J. Nelson, J.E. Harlow, D. Xiong, L.E. Downie, R. Petibon, J.C. Burns, A. Xiao, W.M. Lamanna, J.R. Dahn, J. Electrochem. Soc. 161 (2014) A1818.
[58] J.C. Burns, N.N. Sinha, G. Jain, H. Ye, C.M. VanElzen, W.M. Lamanna, A. Xiao, E. Scott, J. Choi, J.R. Dahn, J. Electrochem. Soc. 159 (2012) A1105.
[59] J. Xia, N.N. Sinha, L.P. Chen, J.R. Dahn, J. Electrochem. Soc. 161 (2013) A264.
[60] M. Gaberscek, J. Moskon, B. Erjavec, R. Dominko, J. Jamnik, Electrochem. Solid-State Lett. 11 (2008) A170.
[61] K. Xu, A. Von Cresce, U. Lee, Langmuir 26 (2010) 11538.
[62] K. Xu, A. von Cresce, J. Mater. Chem. 21 (2011) 9849.
[63] J. Xia, Z. Lu, J. Camardese, J.R. Dahn, J. Power Sources 306 (2016) 516.
[64] J. Self, C.P. Aiken, R. Petibon, J.R. Dahn, J. Electrochem. Soc. 162 (2015) A796.